

An exactly solvable model for fractional quantum Hall effect

G J Sreejith,¹ Abhishek Anand,¹ and J K Jain²

¹Indian Institute of Science Education and Research, Pune 411008, India

²The Pennsylvania State University, 104 Davey Lab, University Park, Pennsylvania 16802, USA

We present a model Hamiltonian for spinless electrons in a magnetic field with strong short-range interaction that lends itself to exact solutions for all low-energy states at arbitrary filling factor $\nu < 1/2p$. The model produces incompressible states at $\nu = n/(2pn + 1)$, where n and p are integers - precisely the filling fractions where fractional quantum Hall effect occurs. We present numerical evidence showing that the fractional quantum Hall ground states of this model are adiabatically connected, and thus topologically equivalent to the Coulomb ground states in the lowest Landau level.

When two-dimensional (2D) electrons are subject to a strong magnetic field, they exhibit the fascinating phenomenon of fractional quantum Hall effect (FQHE)¹, namely quantization of the Hall resistance at $R_H = h/fe^2$ where f is a fraction. Close to a hundred fractions have been observed to date in a variety of 2D electron systems in semiconductor quantum wells and graphene. Several governing themes in contemporary condensed matter physics such as fractional charge² and fractional statistics³, composite fermions⁴, non-Fermi liquids⁵, topological-superconductivity with Majorana particles^{6,7}, and proposals for topological quantum computation⁸ originated in the context of FQHE.

Theoretical investigation of FQHE begins with the Hamiltonian of 2D electrons in a magnetic field:

$$\hat{H} = \sum_{j=1}^N \frac{\hat{\pi}_j^2}{2m_b} + \sum_{j < k=1}^N \hat{V}(|\vec{r}_j - \vec{r}_k|), \quad (1)$$

where $\hat{\pi}_j = \hat{\mathbf{p}}_j + \frac{e}{c}\vec{A}(\hat{\mathbf{r}}_j)$ is the kinetic momentum, $\vec{A}(\vec{r}) = (B/2)(-y, x, 0)$ is the vector potential producing a magnetic field B in the $+z$ direction, m_b is the electron band mass, N is the number of electrons, and \hat{V} is the interaction between the particles. The solutions of the single particle Hamiltonian $\pi^2/2m_b$ are given by

$$\phi_{n,m} = e^{-\frac{r^2}{4}} z^m L_n^m \left(\frac{r^2}{2} \right), \quad E_{n,m} = \left(n + \frac{1}{2} \right) \hbar\omega_c \quad (2)$$

where $n = 0, 1, 2, \dots$ are called Landau levels (LLs), $m = -n, -n + 1, \dots$ is (the z -component of) the angular momentum, $\hbar\omega_c = \hbar eB/m_b c$ is the cyclotron energy, L_n^m is the associated Laguerre polynomial, and we define $z = x - iy$. All lengths are quoted in units of magnetic length $\ell = \sqrt{\hbar c/eB}$. An important parameter is the filling factor, defined as $\nu = N/N_\phi$, where N is the number of particles and $N_\phi = BA/\phi_0$ is the number of flux quanta ($\phi_0 = hc/e$) through the area A occupied by the electrons. The quantized plateau with $R_H = h/fe^2$ occur in a range of electron densities $\nu = f$.

In this manuscript, we discuss an exactly solvable model that contains the physics of FQHE. The traditional theoretical practice since the early works^{2,9} has been to consider the limit $\kappa \equiv V_C/\hbar\omega_c \rightarrow 0$ (here

$V_C = e^2/\epsilon\ell$ sets the Coulomb interaction scale, where ϵ is the dielectric constant of the host material) and restrict the Hilbert space to the lowest LL (LLL), where the interaction energy is the only remaining energy scale. The Coulomb interaction is not exactly solvable. In an important early development, Haldane introduced⁹ a model interaction that obtains Laughlin's wave function at $\nu = 1/3$ as the exact ground state. Other interactions have been designed^{7-9,13-17} for certain specific known wave functions. While these models have greatly added to our understanding, they are not fully solvable, in that each model produces only one fraction, and only the zero energy solutions on the quasihole side are known. The principal result in the present letter is the construction of a single model Hamiltonian for which all low energy eigenstates and eigenenergies at arbitrary $\nu < 1/2p$ can be identified, and which yields FQHE at *all* fractions of the form $n/(2pn + 1)$. A radical departure in our approach is to consider the unconventional limit where the strength of the interaction is infinitely large compared to $\hbar\omega_c$. In this limit, all of the nontrivial physics follows from the restriction to the sector of the many-particle Hilbert space that has zero interaction energy, wherein $\hbar\omega_c$ is the only energy scale. We identify all solutions within the zero interaction energy sector.

The construction of our model interaction is inspired by the composite fermion (CF) physics⁴. In what follows, we will assume fully spin polarized electrons and suppress the spin degree of freedom; generalization to spinful electrons or bosons is straightforward. The composite fermion is the bound state of an electron and $2p$ vortices. In the CF theory, the FQHE state arises from an integer quantum Hall effect (IQHE) state of composite fermions. The electronic wavefunction is obtained by multiplying the IQHE state by the Jastrow factor $\prod_{j < k} (z_j - z_k)^{2p}$, which converts electrons into composite fermions by vortex (or flux) attachment, and also increases the *relative* angular momentum of each pair of electrons, denoted M , by $2p$ units. For two electrons in the n th and n' th LLs, the smallest value of M is $-n - n' + \delta_{n,n'}$. In our construction, we increase M of each pair by $2p$, while preserving their LL indices. In the resulting state the smallest M for a pair with one electron in the n th and another in n' th LLs is $-n - n' + \delta_{n,n'} + 2p$. In other words, pairs

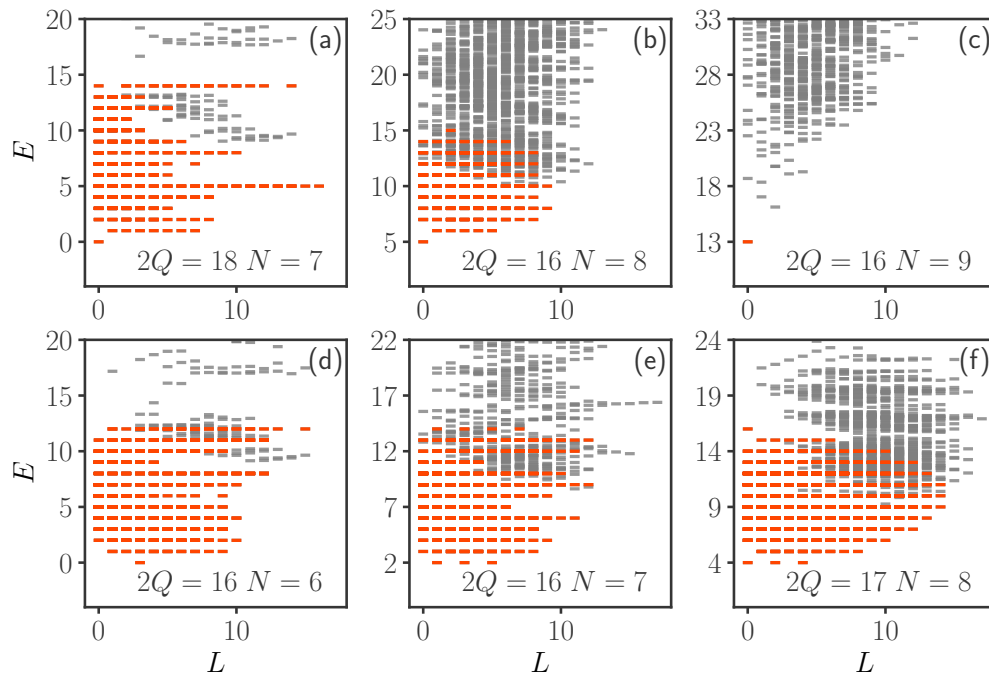


FIG. 1. Spectra of the model Hamiltonian for several representative systems with N particles subjected to $2Q$ flux quanta. All nonzero pseudopotentials of Eq. 5 are identically set to $V_L^{n,n'} = 20\hbar\omega_c$, and the Hilbert space is restricted to the lowest three LLs. N and $2Q$ are displayed on each panel. The energy E is quoted in units of $\hbar\omega_c$, and L is the total orbital angular momentum of the eigenstate. (Here and elsewhere, the zero point kinetic energy of $N\hbar\omega_c/2$ has been removed from E .) Orange markers indicate \mathcal{V}_∞ states with zero interaction energy. (Each orange dash may represent many degenerate eigenstates) Black dashes show eigenstates with non-zero interaction energies; these will be pushed to infinity in the limit $V_L^{n,n'}/\hbar\omega_c \rightarrow \infty$. Panels (a), (b) and (c) show the spectra for systems at filling factors $\nu = 1/3$, $2/5$ and $3/7$; for $\nu = 3/7$ the spectrum has no orange colored excited states, as we have kept only three lowest LLs in our study. Panels (d), (e) and (f) depict the spectra for $(N, 2Q)$ systems for which the ground states consist, respectively, of a single quasihole of $1/3$, two quasiparticles of $1/3$, and two quasiholes of $2/5$.

with $-n - n' + \delta_{n,n'} \leq M < -n - n' + \delta_{n,n'} + 2p$ are absent. We therefore construct an interaction that imposes an energy penalty on these pairs:

$$\hat{V} = \sum_{n \leq n'=0}^{\infty} \sum_{M=-n-n'+\delta_{n,n'}}^{-n-n'+\delta_{n,n'}+2p-1} V_M^{n,n'} |n, n'; M\rangle \langle n, n'; M|. \quad (3)$$

Here $|n, n'; M\rangle$ represents the state of a pair of electrons, one each in n th and n' th LLs, with relative angular momentum M , and $V_M^{n,n'} = \langle n, n'; M | \hat{V} | n, n'; M \rangle$ is the interaction energy of this pair, a generalization of the Haldane pseudopotentials including intra as well as inter LL pairs. (We note that pairs with certain M 's may not be allowed because of exchange symmetry; the corresponding terms are automatically absent in the above Hamiltonian. Also, we have suppressed, for ease of notation, the center-of-mass degree of freedom, which does not affect the pseudopotentials.) The above interaction conserves the LL indices of the particles, and thus also the kinetic energy. The eigenstates of the Hamiltonian can hence be labeled, in addition to the total angular momentum $m_{\text{total}} = \sum_j m_j$, by (N_0, N_1, N_2, \dots) , where N_n is the number of electrons in the n th LL. To describe the low

energy physics of a given fraction at $\nu = n/(2pn + 1)$, terms containing only a finite number of Landau levels need to be kept in the above summation; this restricted interaction is local.

In every case that we numerically studied, we find that the interaction Hamiltonian has a finite gap above its zero energy space. We will now consider the strong interaction limit $V_m^{n,n'}/\hbar\omega_c \rightarrow \infty$, so all eigenstates that do not have zero interaction energy are projected out of the low energy space. The collection of wave functions that have zero interaction energy and are eigenstates of the kinetic energy will be referred to as the \mathcal{V}_∞ space of wavefunctions. The above physics motivates the following construction of \mathcal{V}_∞ wave functions. We denote by $\Phi_{\nu^*}^\alpha$ the distinct kinetic energy eigenstates, labeled by α , of noninteracting fermions at filling factor ν^* ; these are simple Slater determinants. To construct the \mathcal{V}_∞ states, we must increase the relative angular momentum of each pair by $2p$ units in a LL conserving manner. The standard composite-fermionization through multiplication by $\prod_{j < k} (z_j - z_k)^{2p}$ does not conserve the LL index. We

make the *ansatz*:

$$\Psi_{\nu=\frac{\nu^*}{2p\nu^*+1}}^\alpha = \prod_{j<k} (\hat{Z}_j - \hat{Z}_k)^{2p} \times \Phi_{\nu^*}^\alpha \quad (4)$$

where $\hat{Z} = \hat{z} - i(\hat{\pi}_x - i\hat{\pi}_y)/\hbar$ is the guiding center coordinate of a particle. The relation $\nu = \nu^*/(2p\nu^* + 1)$ for the filling factor of the full wave function follows in the standard fashion^{4,18}. That Ψ_ν^α is a \mathcal{V}_∞ state follows from two facts: (i) The guiding center coordinate operator \hat{Z} is similar to the position operator but without any of its matrix elements that scatter between LLs. As a result, \hat{Z} commutes with the kinetic energy. Ψ_ν^α thus has the same kinetic energy as $\Phi_{\nu^*}^\alpha$. (ii) The angular momentum operator for a single particle (Eq. 2) can be written as $\hat{m} = \hat{Z}\hat{Z}^\dagger/2 - \hat{n}$, \hat{n} being the LL index. Guiding center coordinate acts as a raising operator for \hat{m} due to the commutation relation $[\hat{m}, \hat{Z}] = \hat{Z}$. Thus \hat{Z} raises the single particle angular momentum. In the symmetric gauge, the guiding center coordinate has a real space representation of $\hat{Z} \equiv z/2 - 2\partial_{\bar{z}}$. For a pair of particles, $\hat{Z}_1 - \hat{Z}_2$ does not change the center of mass angular momenta, because it commutes with the center of mass $(\hat{z}_1 + \hat{z}_2)/2$ and its momenta. The Jastrow operator $\prod_{j<k} (\hat{Z}_j - \hat{Z}_k)^{2p}$ thus increases the relative angular momentum of every pair of particles by $2p$. Because Ψ_ν^α does not contain pairs with relative angular momenta for which \hat{V} imposes a penalty, Ψ_ν^α has zero interaction energy.

The form of \mathcal{V}_∞ wave functions is extremely restrictive. For example, multiplication of a \mathcal{V}_∞ wave function by a symmetric function $F_S[\{z_j\}]$ produces a non- \mathcal{V}_∞ wave function, as the resulting wave function is not an eigenstate of the kinetic energy (unless the initial wave function happens to be in the LLL, in which case multiplication by $F_S[\{z_j\}]$ produces a linear superposition of zero kinetic energy \mathcal{V}_∞ states). We make the conjecture that the states in Eq. 4 provide a complete basis for the \mathcal{V}_∞ space. This conjecture is equivalent to the statement the spectrum of our model Hamiltonian at any filling factor ν is identical to that of noninteracting fermions at ν^* . Extensive exact diagonalization studies, discussed below, provide a compelling and nontrivial confirmation of the completeness of Ψ_ν^α . As a corollary, our model produces FQHE at $\nu = n/(2pn + 1)$, in complete analogy to the IQHE at $\nu^* = n$.

For exact diagonalization studies, we find it convenient to employ Haldane's spherical geometry⁹, where N electrons move on the surface of a sphere exposed to a total magnetic flux $2Q$ in units of the flux quantum $\phi_0 = h/e$, where $2Q$ is an integer. The single-particle orbitals in the n th LL have angular momentum $l = |Q| + n$. The eigenstates are labeled by the total angular momentum L . The relative pair angular momentum M of the disk geometry corresponds to pair angular momentum $L = 2Q - M$ of the spherical geometry. The interaction of Eq. 3 therefore

translates into

$$\hat{V} = \sum_{n \leq n'=0}^{\infty} \sum_{L=2Q+n+n'-\delta_{n,n'}}^{2Q+n+n'-\delta_{n,n'}} V_L^{n,n'} |n, n'; L\rangle \langle n, n' : L| \quad (5)$$

for the spherical geometry. According to the standard CF theory the interacting system $(N, 2Q)$ of electrons relates to a noninteracting system $(N, 2Q^*)$ of composite fermions with $Q^* = Q - p(N - 1)$. We specialize to $2p = 2$ below.

We have performed exact diagonalization of this Hamiltonian for many systems $(N, 2Q) = (5, 12), (5, 11), (6, 11), (6, 12), (6, 15), (6, 16), (7, 16), (8, 16), (9, 16), (8, 17),$ and $(7, 18)$ in the Hilbert space restricted to the lowest three LLs. See Appendix for details. For many systems the full Hilbert space is prohibitively large, but the calculation becomes possible because we can perform diagonalization in each (N_0, N_1, N_2) sector separately. The resulting spectra shown in Fig. 1 and in the Appendix display IQHE-like structure of bands of states separated by $\hbar\omega_c$. The LL energies on the sphere are $\hbar\omega(n + n(n+1)/2Q)$; but for simplicity, we have assumed that the LL energies depend linearly on the LL index instead, which is strictly true in the limit of the disc geometry $Q \rightarrow \infty$. In our calculations we have set all non-zero pseudopotentials to unity and $V_m^{n,n'} = 1 = 20\hbar\omega_c$; the high-energy parts of the spectra in Fig. 1 also contains states outside the \mathcal{V}_∞ space, which will be pushed to infinity in the limit $V_m^{n,n'}/\hbar\omega_c \rightarrow \infty$. We have tested close to 200 different $(N_0, N_1, N_2, 2Q)$ systems (also see Appendix), and found that in each case the dimension of the \mathcal{V}_∞ space in the exact-diagonalization spectrum agrees exactly with that of noninteracting fermions at $(N_0, N_1, N_2, 2Q^*)$. We note that we have exact wave functions and energies for the ground states, quasiholes, quasiparticles, neutral excitations, and, in fact, all \mathcal{V}_∞ eigenstates. The exact mapping into noninteracting fermions at ν^* is seen to be lost if we set some of the $V_L^{n,n'}$ in Eq. 5 to zero or include additional pseudopotentials; in particular, the inter-LL pseudopotentials are necessary for this program.

Having succeeded in our primary goal of constructing an exactly solvable model that produces FQHE, we turn to the issue of its applicability to experiments. We note that while κ was indeed small in the early experiments¹, FQHE is routinely seen for $\kappa \sim 5 - 7$ in p-doped GaAs²⁰ and ZnO quantum wells²¹ and is seen to survive even upto $\kappa \sim 40$ in high quality AlAs quantum wells²². The limit of strong interactions is thus not entirely unphysical for FQHE. While our model is not intended to produce a quantitative theory of experiments for large κ , we now present evidence that it describes the correct topological phase, which is adiabatically connected to the Coulomb state in the LLL. To begin with, our theory reproduces the prominent qualitative features of the phenomenology, namely FQHE at $\nu = n/(2pn + 1)$ and, by extension to the $n \rightarrow \infty$ limit, the compressible Fermi sea-like states⁵ at $\nu = 1/2p$. The wave functions

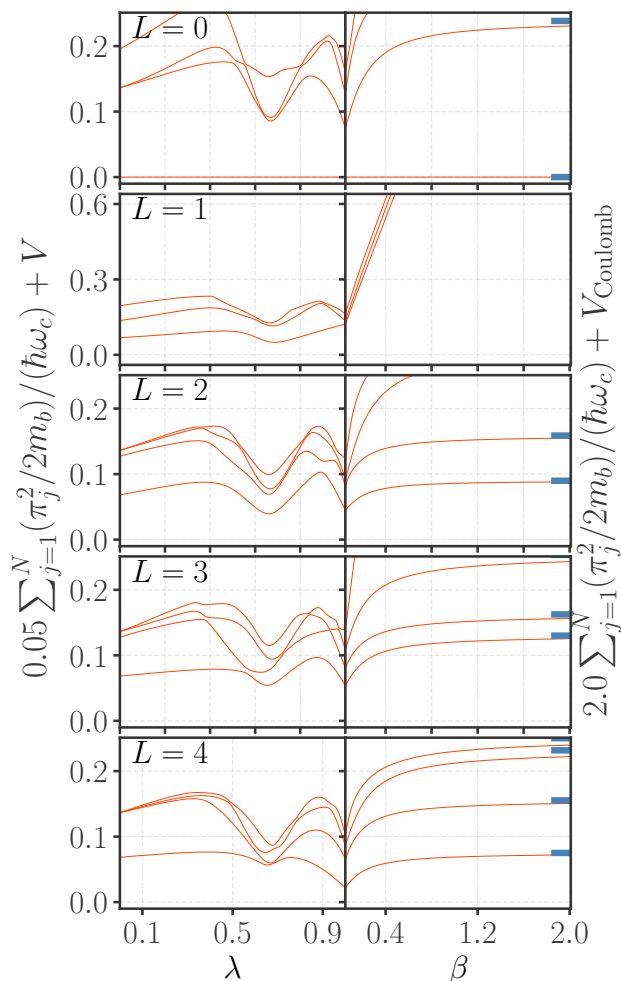


FIG. 2. Demonstration of adiabatic continuity between the ground state and the low energy neutral excitations of the model Hamiltonian and the lowest Landau level Coulomb Hamiltonian for $N = 6$ particles at $\nu = 2/5$. The Hamiltonian is defined by $\hat{H} = \beta \sum_{j=1}^N (\hat{\pi}_j^2 / 2m_b) / (\hbar\omega_c) + (1 - \lambda)\hat{V} + \lambda\hat{V}_{\text{Coulomb}}$ where \hat{V} is the model interaction of Eq. 5 with all of the nonzero pseudopotentials set to unity, \hat{V}_{Coulomb} is the Coulomb interaction, and all energies are quoted in units of $e^2/\epsilon\ell$. At each λ and β , the spectrum has been vertically shifted to set the $L = 0$ ground state energy to 0. The left panels show the evolution of the low-lying eigenstates as λ is varied from 0 to 1 with $\beta = 0.05$. The right panels show the evolution as β is changed from 0.05 to 2.0 with $\lambda = 1$. The lowest three LLs are included in our calculation. The different rows indicate spectra in different angular momentum (L) sectors. The left most spectra ($\lambda = 0$) are for our model interaction, whereas the right-most spectra are for the Coulomb interaction with a high cyclotron energy. The solid blue dashes at the right-most end show the Coulomb energies in the LLL (i.e. for $\lambda = 1$ and $\beta = \infty$). Adiabatic continuity for the low energy states is seen in all cases; the qualitatively different behavior for $L = 1$ (note the different energy scale for this row), for which the states are pushed to very high energies, captures the absence of a low energy neutral mode in the LLL Coulomb spectrum (see Appendix).

of Eq. 4 also have a structure similar to the Jain CF wave functions $\prod_{j < k} (z_j - z_k)^{2p} \Phi_{\nu^*}^\alpha$. Furthermore, our $\nu = n/(2pn + 1)$ state shares various topological features with the standard CF theory valid for the LLL FQHE. Fractional charge of $e^* = e/(2pn + 1)$ for the quasiparticles follows from the presence of gap at a fractional ν , but can also be deduced from the mapping into $2Q^* = 2Q - 2p(N - 1)$ (see Ref.¹⁸). The one-to-one correspondence with IQHE implies that the excitations obey Abelian braid statistics, because the wave function is uniquely determined by specifying the positions of the quasiparticles (which correspond, in mapping to ν^* , to electrons in an otherwise empty LL). The edge physics of $\nu = n/(2pn + 1)$ is fully analogous to that at $\nu^* = n$, which has n edge modes. The number of edge modes, also known as the central charge, can be ascertained by thermal Hall measurements^{23,24}. Another topological quantity is the shift S , or the orbital spin²⁵, defined by the relation $2Q = \nu^{-1}N - S$ for the flux where FQHE states occur in the spherical geometry. Our model produces the same shift, $S = n + 2p$, as the standard CF theory. The shift is accessible through the measurement of an antisymmetric component of the viscosity tensor, known as the Hall viscosity²⁶ or the Lorentz shear modulus²⁷, which is predicted to be $\eta^A = (\hbar/4)S\rho$, where ρ is the density²⁸⁻³⁰.

We further ask if it is possible to go from our Hamiltonian to the LLL Coulomb Hamiltonian without closing of the gap. In Fig. 2 we show the evolution of the $2/5$ ground state as well as low energy excitations along the following path in the parameter space: We first vary parameters to go from our model interaction (where we set all of the non-zero pseudopotentials to unity) continuously to Coulomb (left panels), and then increase $\hbar\omega_c$ (right panels). Not only does the ground state of our model evolve continuously into the LLL Coulomb ground state, but all $\hbar\omega_c$ and $2\hbar\omega_c$ neutral excitations also evolve into their LLL counterparts without level crossings. It is notable that the $L = 1$ excitation is pushed up to high energies; in the standard CF theory, this state is eliminated by LLL projection³¹. Adiabatic continuity at $\nu = 1/3$ is shown in the Appendix.

In summary, this manuscript reports on an exactly solvable model for the strongly-correlated system of electrons in the FQHE regime. This model, with infinitely strong pairwise interaction, lends itself to exact solution for all low energy eigenstates and eigenenergies for arbitrary filling factors less than $1/2p$. The appealing aspect is that this exactly implements the physics of “noninteracting composite fermions,” in that the spectrum of strongly interacting electrons at ν matches that of noninteracting fermions at a related filling factor ν^* .

Acknowledgments: GJS acknowledges financial support from DST-SERB (India) grant ECR/2018/001781 and IISER-Pune CNRS joint research grant. JKJ acknowledges financial support from the U.S. Department of Energy, Office of Science, Basic Energy Sciences, under Award No. DE-SC0005042. Calculations were performed

with PETSc and SLEPc libraries in the Param Brahma (NSM, IISER Pune) and Param Yuva II (CDAC) su-

percomputing facilities. GJS thanks F Alet for useful discussions.

-
- ¹ D. C. Tsui, H. L. Stormer, A. C. Gossard, *Phys. Rev. Lett.* **48**, 1559 (1982).
² R. B. Laughlin, *Phys. Rev. Lett.* **50**, 1395 (1983).
³ B. I. Halperin, *Phys. Rev. Lett.* **52**, 1583 (1984).
⁴ J. K. Jain, *Phys. Rev. Lett.* **63**, 199 (1989).
⁵ B. I. Halperin, P. A. Lee, N. Read, *Phys. Rev. B* **47**, 7312 (1993).
⁶ N. Read, D. Green, *Phys. Rev. B* **61**, 10267 (2000).
⁷ A. Stern, *Nature* **464**, 187 (2010).
⁸ C. Nayak, S. H. Simon, A. Stern, M. Freedman, S. Das Sarma, *Rev. Mod. Phys.* **80**, 1083 (2008).
⁹ F. D. M. Haldane, *Phys. Rev. Lett.* **51**, 605 (1983).
¹⁰ S. A. Trugman, S. Kivelson, *Phys. Rev. B* **31**, 5280 (1985).
¹¹ J. K. Jain, *Phys. Rev. B* **41**, 7653 (1990).
¹² E. H. Rezayi, A. H. MacDonald, *Phys. Rev. B* **44**, 8395 (1991).
¹³ M. Greiter, X.-G. Wen, F. Wilczek, *Phys. Rev. Lett.* **66**, 3205 (1991).
¹⁴ S. H. Simon, E. H. Rezayi, N. R. Cooper, I. Berdnikov, *Phys. Rev. B* **75**, 075317 (2007).
¹⁵ S. Bandyopadhyay, L. Chen, M. Ahari, G. Ortiz, Z. Nussinov, and A. Seidel, *Phys. Rev. B* **98**, 161118(R) (2018).
¹⁶ S. Bandyopadhyay, G. Ortiz, Z. Nussinov, A. Seidel, *Phys. Rev. Lett.* **124**, 196803 (2020).
¹⁷ S. H. Simon, *Fractional Quantum Hall Effects: New Developments*, B. I. Halperin, J. K. Jain, eds. (World Scientific Pub Co Inc, Singapore, 2020), pp. 377–434.
¹⁸ J. K. Jain, *Composite Fermions* (Cambridge University Press, New York, US, 2007).
¹⁹ See Supplemental Material, which includes a discussion of the guiding center coordinates, matrix elements of the Coulomb and the model interactions in the spherical geometry, additional exact spectra, and counting of the degenerate states.
²⁰ M. B. Santos, Y. W. Suen, M. Shayegan, Y. P. Li, L. W. Engel, and D. C. Tsui, *Phys. Rev. Lett.* **68**, 1188 (1992).
²¹ D. Maryenko, *et al.*, *Nature Commun.* **9**, 4356 (2018).
²² M. Shayegan, private communication (2020).
²³ C. L. Kane, M. P. A. Fisher, *Phys. Rev. B* **55**, 15832 (1997).
²⁴ M. Banerjee, *et al.*, *Nature* **545**, 75+ (2017).
²⁵ X. G. Wen, A. Zee, *Phys. Rev. Lett.* **69**, 953 (1992).
²⁶ J. E. Avron, R. Seiler, P. G. Zograf, *Phys. Rev. Lett.* **75**, 697 (1995).
²⁷ I. V. Tokatly, G. Vignale, *Phys. Rev. B* **76**, 161305(R) (2007).
²⁸ N. Read, *Phys. Rev. B* **79**, 045308 (2009).
²⁹ I. V. Tokatly, G. Vignale, *Journal of Physics: Condensed Matter* **21**, 275603 (2009).
³⁰ S. Pu, M. Fremling, J. K. Jain, *Phys. Rev. Research* **2**, 013139 (2020).
³¹ G. Dev, J. K. Jain, *Phys. Rev. Lett.* **69**, 2843 (1992).

APPENDIX

In Sec. A we introduce guiding center coordinates. The Haldane pseudopotentials are generalized to the problem including many LLs in Sec. B. This is followed by a discussion of the matrix elements for the Coulomb interaction as well as our model interaction in Section C. In Sec. D we present additional spectra from exact diagonalization of our model Hamiltonian. Sec. E gives a large number of examples showing that the counting of states in exact diagonalization matches precisely with our conjecture that maps it into a system of noninteracting fermions. Sec. F connects our model with the LLL Coulomb model for 6 particles at $\nu = 1/3$ by demonstrating adiabatic continuity between the two. (Similar relation is demonstrated for $\nu = 2/5$ in the main text.) We conclude with a discussion of the Trugman-Kivelson model interaction, which obtains a related wave function as the exact ground state at $\nu = 2/5$.

Appendix A: Landau quantization and guiding center coordinates

The Hamiltonian of a particle of mass m and charge $-e$, in a uniform magnetic field in the z direction is given by

$$\hat{H} = \frac{\hat{\pi}^2}{2m_b}, \quad \text{where } \hat{\pi} = \hat{\mathbf{p}} + \frac{e}{c}\mathbf{A}(\hat{\mathbf{r}}), \quad (\text{A1})$$

The kinetic momentum $\hat{\pi}$ satisfies the commutation relations $[\hat{x}_j, \hat{\pi}_i] = i\hbar\delta_{ij}$ similar to the canonical momentum. The components of $\hat{\pi}$ however do not commute; we have $[\hat{\pi}_x, \hat{\pi}_y] = -i\frac{\hbar^2}{\ell^2}$ where ℓ is the magnetic length $\sqrt{\hbar c/eB}$. The Hamiltonian in Eq. A1 is a thus quadratic function of canonically conjugate variables, reminiscent of the quantum harmonic oscillator. Following arguments analogous to those in the quantum harmonic oscillators, the Hamiltonian can be expressed as $\hbar\omega_c(\hat{a}^\dagger\hat{a} + 1/2)$ where the energy ladder operator defined as

$$\hat{a}^\dagger = \frac{\ell}{\sqrt{2}\hbar}(\hat{\pi}_x + i\hat{\pi}_y) \quad (\text{A2})$$

satisfies a commutation relation $[\hat{a}, \hat{a}^\dagger] = 1$. The operator raises the energy of a state it acts on by $\hbar\omega_c$ on account of its commutation relation with the Hamiltonian: $[H, \hat{a}^\dagger] = \hbar\omega_c\hat{a}^\dagger$. The cyclotron frequency ω_c is given by $eB/m_b c$.

Action of the energy ladder operator covers only part of the degrees of freedom. This can be seen upon exploring the dynamics of the position operator $\hat{z} = \hat{x} - i\hat{y}$.

$$\partial_t \hat{z} = \frac{1}{i\hbar} [\hat{z}, \hat{H}] = \frac{1}{m} (\hat{\pi}_x - i\hat{\pi}_y) = \frac{\sqrt{2}\hbar}{m\ell} \hat{a} \quad (\text{A3})$$

The time evolution of the position resembles the time evolution of a :

$$\partial_t \hat{a} = \frac{1}{i\hbar} [\hat{a}, H] = -i\omega_c \hat{a} \quad (\text{A4})$$

These suggest that a suitable linear combination of \hat{z} and a , namely

$$\hat{Z} = \hat{z} - i\sqrt{2}\ell\hat{a}, \quad (\text{A5})$$

is time independent, i.e. commutes with the Hamiltonian. This constant of motion is called the guiding center coordinate. Action of this operator changes a state without altering its energy, indicating that it affects degrees of freedom different from those captured by the energy ladder operators. It is easily verified that \hat{Z} and \hat{a} together satisfy the following commutation relations

$$[\hat{a}, \hat{a}^\dagger] = 1; [\hat{a}, \hat{Z}] = [\hat{a}^\dagger, \hat{Z}] = 0; [\hat{Z}^\dagger, \hat{Z}] = 2\ell^2 \quad (\text{A6})$$

The space in which this algebra acts is spanned by the energy states of the form

$$|n, s - n\rangle = \frac{(\hat{a}^\dagger)^n (\hat{Z}/\sqrt{2}\ell)^s}{\sqrt{n!} \sqrt{s!}} |0, 0\rangle; n, s = 0, 1, \dots \infty \quad (\text{A7})$$

where $|0, 0\rangle$ is annihilated by both \hat{a} and \hat{Z}^\dagger . This state has an energy $(n + 1/2)\hbar\omega_c$ and angular momentum $m = s - n$. The LL index $n = 0, 1, 2, \dots$ and the angular momentum $m = -n, -n + 1, \dots \infty$ are eigenvalues of the LL index operator $\hat{n} = \hat{a}^\dagger \hat{a}$ and the angular momentum operator $\hat{m} = \hat{Z} \hat{Z}^\dagger / 2\ell^2 - \hat{n}$. The guiding center coordinates \hat{Z} and \hat{Z}^\dagger act as raising and lowering operators for the angular momentum.

The discussion so far is gauge independent. Guiding center coordinate \hat{Z} can be written in real space representation once a choice for the gauge \mathbf{A} has been made. In the symmetric gauge $\mathbf{A} \equiv B(-y, x)/2$, the guiding center coordinate is

$$\begin{aligned} \hat{Z} &= \hat{z} - i\sqrt{2}\ell\hat{a} = \hat{z} - i\frac{\ell^2}{\hbar} (\hat{\pi}_x - i\hat{\pi}_y) \\ &\equiv \frac{x - iy}{2} - \ell^2 (\partial_x - i\partial_y) = \frac{z}{2} - 2\ell^2 \partial_{\bar{z}} \end{aligned} \quad (\text{A8})$$

Appendix B: Generalized Haldane pseudopotentials

Let us denote by $|n_1 n_2; \tilde{M} M\rangle$ the state of two electrons that occupy the n_1 th and n_2 th LLs and have a relative angular momentum M and center of mass angular momentum \tilde{M} . It is evident that the state labeled by these quantum numbers, if allowed by symmetry, is unique. It can be generated by exact diagonalization of a rotationally invariant interaction in the appropriate Hilbert space. In fact, given the wave function for the minimum

relative angular momentum pair for a given n_1 and n_2 , the states may be generated by repeated application of $(\hat{Z}_1 \pm \hat{Z}_2)$. More specifically, we write

$$|n_1 n_2; \tilde{M} M\rangle \equiv (\hat{Z}_1 + \hat{Z}_2)^{\tilde{M}} (\hat{Z}_1 - \hat{Z}_2)^M \times |(n_1, -n_1)(n_2, -n_2 + \delta_{n_1 n_2})\rangle \quad (\text{B1})$$

where $|(n_1, -n_1)(n_2, -n_2 + \delta_{n_1 n_2})\rangle = |n_1, -n_1\rangle |n_2, -n_2 + \delta_{n_1 n_2}\rangle$ is the two-particle state with the minimum relative angular momentum and zero center of mass momentum.

An interaction is characterized by the generalized Haldane's pseudopotentials

$$V_M^{n_1 n_2; n'_1 n'_2} = \langle n'_1 n'_2; \tilde{M} M | \hat{V}(|\vec{r}_1 - \vec{r}_2|) | n_1 n_2; \tilde{M} M \rangle \quad (\text{B2})$$

The pseudopotential does not depend on \tilde{M} , but, in general, has matrix elements involving LL transitions. Our model interaction preserves LLs, and thus keeps only the diagonal pseudopotentials $V_M^{n_1 n_2; n_1 n_2} \equiv V_M^{n_1 n_2}$.

Appendix C: Interaction Hamiltonians in the spherical geometry

A general two-particle interaction between particles on a sphere can be written as follows

$$\sum_{l_1, l_2=|Q|}^{\infty} \sum_{m_1=-l_1}^{l_1} \sum_{m_2=-l_2}^{l_2} c_{l_1 m_1}^\dagger c_{l_2 m_2}^\dagger V_{12; 1'2'} c_{l_2 m'_2} c_{l_1 m'_1} \quad (\text{C1})$$

where $V_{12; 1'2'}$ is a shorthand for the matrix element of the interactions between two-particle states ie

$$V_{12; 1'2'} \equiv \langle (l_1, m_1), (l_2, m_2) | \hat{V}(|l'_1, m'_1\rangle, |l'_2, m'_2\rangle) \rangle \quad (\text{C2})$$

where $|(l_1, m_1), (l_2, m_2)\rangle$ is a two-particle state with particles occupying m_1 and m_2 angular momentum states in the LLs l_1 and l_2 respectively.

Any two-particle interaction is fully characterized by its matrix elements. In the remainder of this section, we first describe the calculation of the matrix elements for the Coulomb interaction¹, as well as for our model interaction, for electrons residing on the surface of a sphere.

1. Coulomb interaction

The Coulomb interaction between particles on the surface of a sphere is $1/r$ where r is the chord distance $|\mathbf{r}_a - \mathbf{r}_b|$ between the positions $\mathbf{r}_a \equiv (\theta_a, \phi_a)$ and $\mathbf{r}_b \equiv (\theta_b, \phi_b)$. The radius of the sphere is $R = \sqrt{Q}$ in units of the magnetic length $\ell = \sqrt{\hbar c / eB}$, $B = 2Q\Phi_0 / 4\pi R^2$ is the field strength on the surface of the sphere, and $2Q$ is the (integer) number of flux quanta emanating from a monopole placed at the center of the sphere. Eigenstates of the single particle Hamiltonian $\hat{\pi}^2 / 2m_b$ in this geometry are called the monopole spherical harmonics

Y_{Qlm} .^{2,3} The quantity $l = |Q| + n$ is the angular momentum of the orbitals in the n th LL ($n = 0, 1, \dots$) and $m = -l, -l + 1, \dots, l$ labels the degenerate states in the n th LL.

The Coulomb potential can be expanded in terms of the Legendre polynomials as

$$\frac{1}{r} = \frac{1}{\sqrt{Q}} \sum_{l=0}^{\infty} P_l(\cos \theta),$$

where θ is the angle subtended by \mathbf{r}_a and \mathbf{r}_b at the origin. The Legendre Polynomial can be expressed in terms of the monopole spherical harmonics (Eq. 14.30.9 of Ref. 4) resulting in the expression

$$\frac{1}{r} = \frac{1}{\sqrt{Q}} \sum_{l=0}^{\infty} \frac{4\pi}{2l+1} \sum_{m=-l}^l Y_{0lm}^*(a) Y_{0lm}(b). \quad (\text{C3})$$

Here the arguments a and b of the monopole Harmonics are a short-hand notation to represent the coordi-

nates (θ_a, ϕ_a) and (θ_b, ϕ_b) . The matrix element (Eq. C2) of the Coulomb interaction between a pair of (antisymmetrized) two-particle fermionic states $|(l_1, m_1)(l_2, m_2)\rangle$ and $|(l'_1, m'_1)(l'_2, m'_2)\rangle$ is given by

$$V_{12;1'2'} \equiv V_{(l_1 m_1)(l_2 m_2)}^{(l'_1 m'_1)(l'_2 m'_2)} - V_{(l_1 m_1)(l_2 m_2)}^{(l'_2 m'_2)(l'_1 m'_1)} + V_{(l_2 m_2)(l_1 m_1)}^{(l'_2 m'_2)(l'_1 m'_1)} - V_{(l_2 m_2)(l_1 m_1)}^{(l'_1 m'_1)(l'_2 m'_2)} \quad (\text{C4})$$

where

$$V_{(l_1 m_1)(l_2 m_2)}^{(l'_1 m'_1)(l'_2 m'_2)} = \int Y_{Ql_1 m_1}^*(a) Y_{Ql_2 m_2}^*(b) V(r) Y_{Ql'_1 m'_1}(a) Y_{Ql'_2 m'_2}(b) d\Omega_a d\Omega_b. \quad (\text{C5})$$

Theorems 1 and 3 from Ref 2 can be used to evaluate the integrals involved in terms of Wigner 3j symbols, yielding the following expression for $V_{(l_1 m_1)(l_2 m_2)}^{(l'_1 m'_1)(l'_2 m'_2)}$:

$$\sum_{l=0}^{\infty} \nu_l \sum_{m=-l}^l \sqrt{(2l_1+1)(2l_2+1)(2l'_1+1)(2l'_2+1)(-1)^{2Q+m_1+m_2+l_1+l_2+l'_1+l'_2}} \begin{pmatrix} l_1 & l & l'_1 \\ -m_1 & -m & m_1 \end{pmatrix} \begin{pmatrix} l_2 & l & l'_2 \\ -m_2 & m & m_2 \end{pmatrix} \begin{pmatrix} l_1 & l & l'_1 \\ -Q & 0 & Q \end{pmatrix} \begin{pmatrix} l_2 & l & l'_2 \\ -Q & 0 & Q \end{pmatrix} \quad (\text{C6})$$

where $\nu_l = 1/\sqrt{Q}$. The series can be summed numerically to obtain the Coulomb matrix elements. The series terminates at sufficiently large l as the Wigner 3j symbols are nonzero only for those arguments that satisfy certain constraints (Sec 34.2 of Ref 4).

2. Model interaction

Matrix element (Eq. C2) of the model interaction introduced in this work can be obtained by sandwiching the interaction shown in Eq. 5 of the main text between two-particle states. For convenience we reproduce the interaction in full detail here

$$\hat{V} = \sum_{l_1 < l_2 = 0}^{\infty} \sum_{L=2Q+l_1+l_2-\delta_{l_1 l_2}}^{2Q+l_1+l_2-\delta_{l_1 l_2}} \sum_{L_z=-L}^L V_L^{l_1, l_2} \times |l_1, l_2, L, L_z\rangle \langle l_1, l_2, L, L_z| \quad (\text{C7})$$

Here $|l_1, l_2, L, L_z\rangle$ is the unique two-particle state of total angular momentum quantum number L and z -component angular momentum L_z , constructed from two particles in the $n_1 = l_1 - Q$ and $n_2 = l_2 - Q$ LLs. Note that we have restored the sum over L_z which was omitted in Eq. 5 of the main text for brevity. With this, the

matrix element (Eq. C2) between the two-particle states $|(l'_1, m'_1), (l'_2, m'_2)\rangle$ and $|(l_1, m_1), (l_2, m_2)\rangle$ is given by

$$\delta_{(l_1, l_2)(l'_1, l'_2)} V_L^{l_1, l_2} C_{(l_1, m_1)(l_2, m_2)}^{L, L_z} C_{(l_1, m'_1)(l_2, m'_2)}^{L, L_z} \quad (\text{C8})$$

where $C_{(l_1, m_1)(l_2, m_2)}^{L, L_z}$ is the Clebsch Gordan coefficient.

Appendix D: Spectra from Exact Diagonalization

We have shown several spectra for our model Hamiltonian in the main text. Figure 3 shows additional representative spectra, all evaluated within the Hilbert space of the lowest 3 LLs. All nonzero pseudopotentials of the interaction are set to 20 in units of $\hbar\omega_c = 1$. The zero interaction energy states (i.e. the states belonging to \mathcal{V}_∞) are indicated using orange markers and the remaining states are indicated with gray markers; the latter will be pushed to infinity in the limit where the interaction is taken to be infinitely strong. Panel (a) shows the system $(N, 2Q) = (6, 11)$, which maps into noninteracting fermion system $(N, 2Q^*) = (6, 1)$. Here, the spectrum contains a single incompressible ground state with $(N_0, N_1, N_2) = (2, 4, 0)$, followed by neutral excitations at $\hbar\omega_c$ at $L = 1, 2, 3, 4$ in the $(N_0, N_1, N_2) = (2, 3, 1)$ sector. Panel (b) shows the spectrum of $(N, 2Q) = (5, 11)$,

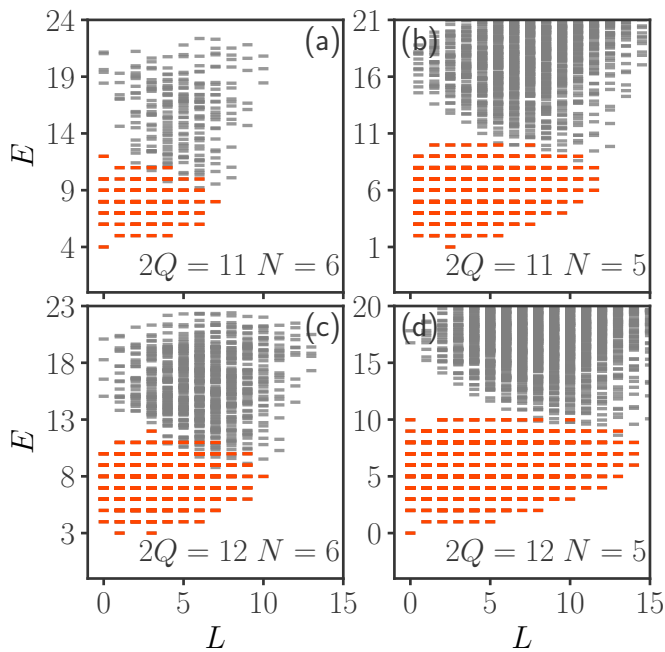


FIG. 3. Spectra for our model interaction for different $(N, 2Q)$ systems on the sphere. Orange markers indicate eigenstates with zero interaction energies. $\hbar\omega$ is set to 1 and all non-zero pseudopotentials are set to 20. The black dashes show eigenstates that have nonzero interaction energy, i.e. are outside the \mathcal{V}_∞ sector.

which maps into $(N, 2Q^*) = (5, 3)$. The ground state corresponds to $(N_0, N_1, N_2) = (4, 1, 0)$, i.e. describes a single quasiparticle of the $1/3$ state. The angular momentum of this quasiparticle is predicted to be $L = 5/2$. Panel (c) shows the spectrum of $(N, 2Q) = (6, 12)$, which maps into $(N, 2Q^*) = (6, 2)$. The ground state sector, with $(N_0, N_1, N_2) = (3, 3, 0)$, has two quasiholes of the $2/5$ state, each carrying an angular momentum of $l = 2$. Addition of their angular momentum produces low energy states at total $L = 1, 3$, precisely as seen in panel (c). Panel (d) shows the $(N, 2Q) = (5, 12)$ which corresponds to the one filled LL state $(N, 2Q^*) = (5, 4)$. In all cases low energy states show same structure as what is expected in the LLL Coulomb spectrum.

Appendix E: Counting of \mathcal{V}_∞ states

In this section we present results comparing the number of numerically obtained zero energy \mathcal{V}_∞ states $(N, 2Q)$ with the dimension of the Hilbert space of the corresponding noninteracting system at $(N, 2Q^*)$, with $2Q^* = 2Q - 2p(N - 1)$. All exact diagonalizations are performed in the space of the lowest three LLs.

\mathcal{V}_∞ states are constructed by acting $\hat{J} = \prod_{i < j=1}^N (\hat{Z}_i - \hat{Z}_j)^{2p}$ on the slater determinant states with a fixed number of particles (N_0, N_1, N_2) in each LL. Maximum angular momenta of the particles in the slater determinant is

less than that in the corresponding \mathcal{V}_∞ state as the Jastrow factor \hat{J} adds an angular momentum of $2p(N - 1)$ for each particle.

While the states constructed in this manner definitely belong to the \mathcal{V}_∞ sector, one can ask: (i) Do different rearrangements of particles in a given (N_0, N_1, N_2, \dots) sector produce linearly independent \mathcal{V}_∞ states? This seems likely, as the resulting states are very complex, but we do not have an analytic proof. (ii) Are there other other \mathcal{V}_∞ states that are not captured by this construction? We have failed to find such states, but, rigorously speaking, cannot rule out this possibility a priori.

We have conjectured that the states obtained in this fashion are all linearly independent and provide a complete basis for the \mathcal{V}_∞ space. In other words, in the spherical geometry, the \mathcal{V}_∞ eigenstates in exact diagonalization spectrum of $(N, 2Q)$ have an exact one-to-one correspondence with the eigenstates of noninteracting fermions at $(N, 2Q^*)$, with $2Q^* = 2Q - 2p(N - 1)$. Alternatively: (i) all \mathcal{V}_∞ states are of this form (or linear combinations of them), and (ii) \mathcal{V}_∞ states constructed from different slater determinant states are linearly independent, i.e., the action of \hat{J} does not annihilate any wave function.

We provide convincing numerical evidence for this conjecture by explicitly diagonalizing our model interaction in various (N_0, N_1, N_2) sectors at several values of $2Q$ to obtain their zero interaction energy eigenstates. The results are shown in the tables II, I and III. In every case the number matches the number of different slater determinant states at $2Q^*$ in the (N_0, N_1, N_2) sector. Only the number of the $L_z = 0$ states is shown. In addition to the cases shown in the tables, the expected counting is obtained for the $(N, 2Q) = (9, 16)$ system, where only a single \mathcal{V}_∞ state occurs in the sector $(N_0 = 1, N_1 = 3, N_2 = 5)$, corresponding to the $\nu = 3/7$ ground state. The one-to-one correspondence is seen for all cases we have studied.

Zero energy space dimensions were computed using Krylov-Schur algorithm⁵ with large Krylov subspace dimensions.

Appendix F: Adiabatic continuity at $\nu = 1/3$

In the main text, we have shown how the low-energy spectrum of our model Hamiltonian at $\nu = 2/5$ evolves into the low-energy spectrum of the Coulomb interaction in the LLL under a continuous deformation of the Hamiltonian. We demonstrate the same for $\nu = 1/3$ in this section.

Figure 4 shows how the low-energy spectrum of the model Hamiltonian (in the spherical geometry) evolves

N_0, N_1, N_2	$2Q = 11$	$2Q = 12$
0,0,5	6	12
0,1,4	41	74
0,2,3	80	146
0,3,2	56	108
0,4,1	14	31
0,5,0	1	3
1,0,4	29	56
1,1,3	130	246
1,2,2	165	322
1,3,1	70	147
1,4,0	9	21
2,0,3	35	76
2,1,2	103	222
2,2,1	79	178
2,3,0	17	40
3,0,2	13	36
3,1,1	23	64
3,2,0	9	26
4,0,1	1	5
4,1,0	1	5
5,0,0	0	1

TABLE I. The number of independent $L_z = 1/2$ zero interaction energy (\mathcal{V}_∞) eigenstates in exact-diagonalization spectra for many different (N_0, N_1, N_2) sectors for several values of $2Q$. The total number of particles is $N = 5$. In every single case, the number of numerically obtained zero interaction energy eigenstates matches exactly with the number of Slater determinant states for noninteracting electrons in the (N_0, N_1, N_2) sector at $2Q^* = 2Q - 2(N - 1)$.

as the Hamiltonian is continuously changed to the LLL Coulomb Hamiltonian along a particular path in the parameter space. Each row of the figure shows the evolution of the spectrum within a single total angular momentum sector. The Hamiltonian is parametrized by two parameters λ and β as follows

$$\hat{H}(\beta, \lambda) = \frac{\beta}{\hbar\omega_c} \sum_{i=1}^N \frac{\hat{\pi}_i^2}{2m} + (1 - \lambda)\hat{V} + \lambda\hat{V}_{\text{Coulomb}} \quad (\text{F1})$$

where \hat{V} is the model Hamiltonian and \hat{V}_{Coulomb} is the Coulomb Hamiltonian. All energies are quoted in units of $e^2/(\epsilon\ell)$. Nonzero pseudopotentials of the model Hamiltonian are all set to 1.

The left panels show the spectral flow as λ is changed from 0 to 1 with $\beta = 0.05$. At the left end, the Hamiltonian $\hat{H}(\beta = 0.05, \lambda = 0)$ represents a system with a small

N_0, N_1, N_2	$2Q = 11$	$2Q = 12$	$2Q = 15$	$2Q = 16$
6,0,0	0	0	1	1
5,1,0	0	0	6	19
4,2,0	0	0	44	108
5,0,1	0	0	6	21
3,3,0	0	2	106	236
4,1,1	0	0	106	265
2,4,0	1	3	100	210
3,2,1	0	10	452	978
4,0,2	0	0	59	143
1,5,0	0	1	34	74
2,3,1	4	28	656	1328
3,1,2	0	13	550	1165
0,6,0	0	0	4	8
1,4,1	2	15	334	674
2,2,2	14	74	1372	2662
3,0,3	0	5	186	393
0,5,1	0	1	48	102
1,3,2	18	74	1086	2054
2,1,3	12	61	1028	1971
0,4,2	3	13	236	452
1,2,3	34	118	1396	2556
2,0,4	3	13	236	452
0,3,3	12	40	470	858
1,1,4	18	61	708	1292
0,2,4	14	40	410	728
1,0,5	2	9	114	214
0,1,5	4	13	146	264
0,0,6	1	1	18	32

TABLE II. The number of independent $L_z = 0$ zero interaction energy (\mathcal{V}_∞) eigenstates in exact-diagonalization spectra for many different (N_0, N_1, N_2) sectors for several values of $2Q$. The total number of particles is $N = 6$. In every single case, the number of numerically obtained zero interaction energy eigenstates matches exactly with the number of Slater determinant states for noninteracting electrons in the (N_0, N_1, N_2) sector at $2Q^* = 2Q - 2(N - 1)$.

cyclotron gap of 0.05 and particles interacting via the model Hamiltonian \hat{V} . At the right end of the left panels, $\hat{H}(\beta = 0.05, \lambda = 1)$ represents the Hamiltonian of the system with the same cyclotron gap but instead interacting via the Coulomb interaction. The right panels show the spectral transformation as β is varied from 0.05 to 2 keeping $\lambda = 1$. At the rightmost end, on account of the

N_0, N_1, N_2	$2Q = 16$	N_0, N_1, N_2	$2Q = 16$
7,0,0	0	0,2,5	210
0,7,0	1	3,0,4	108
0,0,7	4	1,5,1	91
6,1,0	0	0,4,3	236
6,0,1	0	0,3,4	344
1,6,0	5	1,1,5	356
0,6,1	7	4,2,1	91
1,0,6	38	4,1,2	114
0,1,6	52	2,4,1	286
5,2,0	3	1,4,2	520
5,0,2	4	3,3,1	286
2,5,0	26	2,1,4	700
0,5,2	68	1,2,4	1016
4,3,0	21	3,1,3	482
5,1,1	7	1,3,3	1136
2,0,5	108	3,2,2	628
3,4,0	40	2,3,2	1022
4,0,3	38	2,2,3	1372

TABLE III. The number of independent $L_z = 0$ zero interaction energy (V_∞) eigenstates in exact-diagonalization spectra for different (N_0, N_1, N_2) sectors within the $(N, 2Q) = (7, 16)$ system. In every single case, the number of numerically obtained zero interaction energy eigenstates matches exactly with the number of slater determinant states of noninteracting electrons in the (N_0, N_1, N_2) sector at $2Q^* = 2Q - 2(N - 1)$.

relatively large cyclotron energy, particles predominantly reside in the LLL. The spectrum here closely matches the spectrum of the Coulomb interaction for particles strictly confined to the LLL, which corresponds to the case of infinite cyclotron gaps (Fig 5 (bottom)). The LLL Coulomb energies are shown as blue dashes on the right end of the panel. All energies in all the plots are measured relative to the energy of the $L = 0$ ground state, which remains the global ground state throughout the evolution.

The uniform ground state of the model Hamiltonian ($L = 0$ sector shown in the top panels) is adiabatically connected to the ground state of the Coulomb interaction in the LLL. As discussed below, the low energy states also appear to be adiabatically connected to each other. Just above the ground state in the LLL Coulomb spectrum (Fig 5) is a neutral excitation mode⁶ occurring at momenta $L = 2$ to $L = N$ (one state at each of these angular momenta). These states correspond to particle-hole excitations over the ground state. A similar mode is also present at the corresponding angular momenta in the spectrum of our model Hamiltonian separated by the cyclotron gap (Fig 5 top panel). The states in the $L \geq 3$

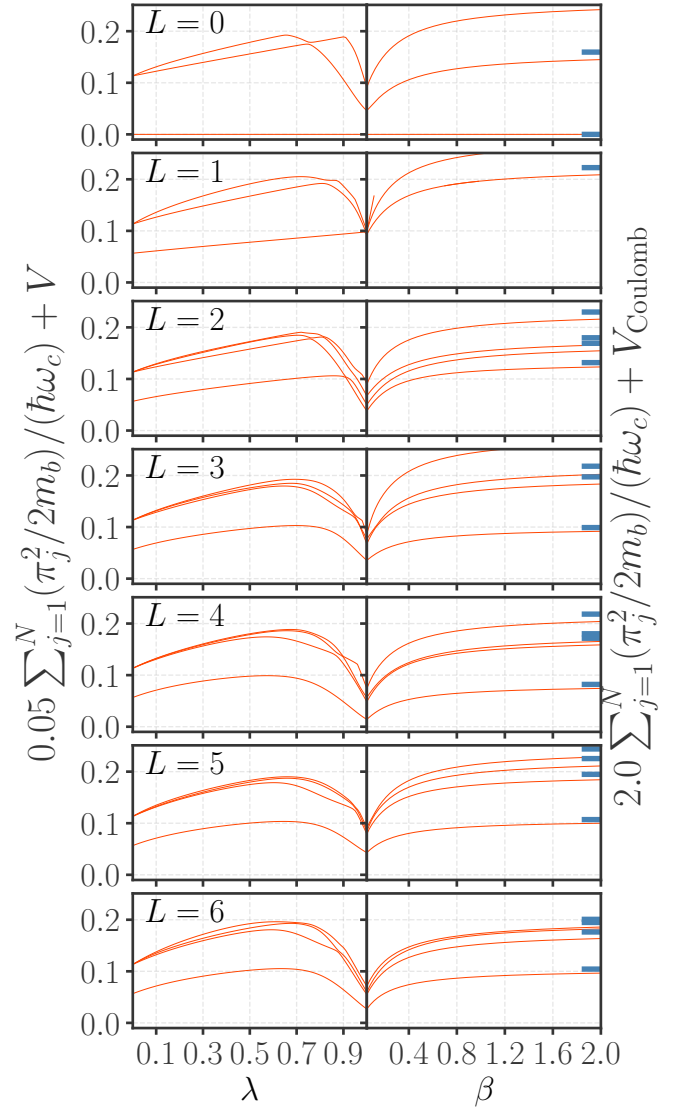


FIG. 4. Demonstration of adiabatic connectivity of low energy eigenstates of our model Hamiltonian and the those of the LLL Coulomb Hamiltonian for a six particle system at $\nu = 1/3$. The form of Hamiltonian is $\hat{H} = \beta \sum_{j=1}^N (\hat{\pi}_j^2 / 2m_b) / (\hbar\omega_c) + (1 - \lambda)\hat{V} + \lambda\hat{V}_{\text{Coulomb}}$. Three LLs are included in the calculation. The left panels show the change in the spectra as λ changes from 0 to 1 keeping $\beta = 0.05$ and the right panels show the variation as β changes from 0.05 to 2. Different rows show spectra in different L sectors. All the energies are relative to ground state of $L = 0$. The ground state of the model Hamiltonian is adiabatically connected to the ground state of the LLL Coulomb Hamiltonian. The same is true of the neutral excitations, with the exception of a level crossing for $L = 2$.

sectors in these two Hamiltonians are adiabatically connected as can be seen in the corresponding panels of Fig 4. Note that the particle-hole pairs forming the neutral mode are far separated at larger angular momenta. At $L = 2$, where the particle-hole pair are spatially closer to one another, there is a level crossing as the spectrum

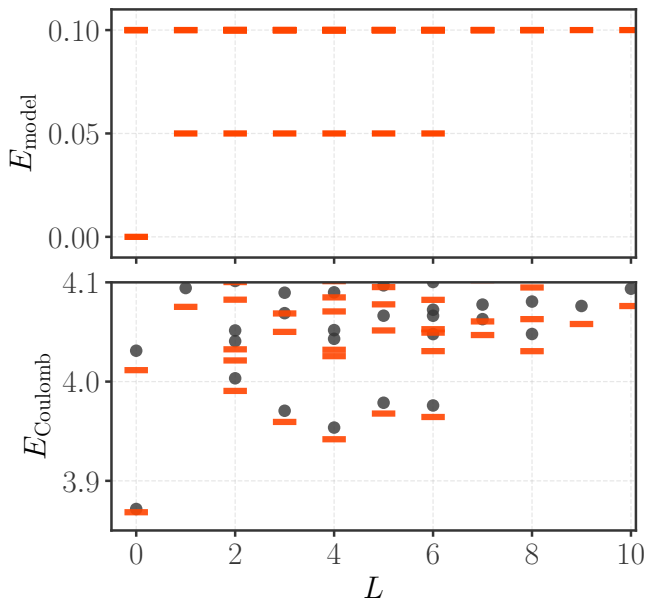


FIG. 5. Low energy spectra of the Hamiltonians $\hat{H}(\beta = 0.05, \lambda = 0)$ (top) and $\hat{H}(\beta = 2.0, \lambda = 1)$ (bottom, dashes) for a system of $N = 6$ particles and $2Q = 15$. Dots in the bottom figure represent the LLL Coulomb spectrum.

evolves. Proximity of the particle-hole pair results in the spectrum in this sector to be sensitive to short range details of the Hamiltonian. An $L = 1$ state is present in the neutral mode of the model Hamiltonian spectrum but is absent in the LLL Coulomb spectrum. As the Hamiltonian is varied, this state drifts to higher energies. Note that in the CF construction of the neutral mode, the $L = 1$ exciton state vanishes only if strictly projected to lowest Landau level.

Appendix G: Trugman-Kivelson Hamiltonian

Trugman and Kivelson⁷ (TK) introduced the interaction

$$V_{\text{TK}}(r) = \nabla^2 \delta(r), \quad (\text{G1})$$

which obtains Laughlin’s wave function as the unique solution at $\nu = 1/3$ in the LLL Hilbert space. Interestingly, if one sets the lowest two LLs degenerate while sending the remaining higher LLs to infinity, then the

unprojected Jain state at $\nu = 2/5$:

$$\Psi_{2/5}^{\text{CF}} = \prod_{i < j=1}^N (z_i - z_j)^2 \Phi_2(\{z_i\}), \quad (\text{G2})$$

where $\Phi_2(\{z_i\})$ is the spin polarized integer quantum Hall state at filling fraction 2, appears as the unique zero-energy ground state for the TK interaction^{8,9}. This state occurs at flux $2Q = 5N/2 - 4$ on the sphere. It is interesting to ask in what sense the TK interaction is different from the one considered here.

On the sphere, the TK interaction can be expanded in spherical Harmonics as (compare with Eq. C3)

$$\nabla^2 \delta(\mathbf{r}_a - \mathbf{r}_b) = - \sum_{l=0}^{\infty} \sum_{m=-l}^l \frac{l(l+1)}{Q} Y_{0lm}(a) Y_{0lm}^*(b) \quad (\text{G3})$$

where we have expanded the Dirac delta function in monopole spherical harmonics (Eqn 1.17.25 of Ref 4). The matrix elements of the TK Hamiltonian can be found in a manner similar to that for the Coulomb Hamiltonian and have the same form as Eq. C4 and Eq. C6 but with $\nu_l = -l(l+1)(2l+1)/4\pi Q$.

It is interesting to ask in what way the TK Hamiltonian is different from ours. To address this, we consider the system of particles living in the Hilbert space of the two lowest LLs. Our model Hamiltonian introduced in this work imposes an energy penalty on (i) all two-particle states of relative angular momenta $L = 2Q + 1$ and $2Q$ on the sphere; and on (ii) the unique multiplet of two-particle states of angular momenta $2Q - 1$ in the LLL.

Like our model Hamiltonian, the TK Hamiltonian also imposes an energy penalty on all states in the $L = 2Q + 1$ and $2Q$ sectors. In the $L = 2Q - 1$ sector, however, it imposes a penalty on a particular two-particle multiplet in the three dimensional (multiplet) space of the $L = 2Q - 1$ states. This multiplet is a linear combination of two-particles states in multiple LLs. That makes TK Hamiltonian LL non-conserving. The “forbidden” two-particle multiplet of the TK Hamiltonian in the $L = 2Q - 1$ sector can be inferred from numerically studying the two-particle spectrum of the TK Hamiltonian, using the matrix elements evaluated as described above.

Figure 6 depicts spectra for the TK Hamiltonian for the same $(N, 2Q)$ systems as in Fig. 3. Only the two lowest LLs (taken as degenerate) are included in the diagonalization. The unique zero energy state occurring in the panel (a) is identical to the Jain unprojected wave function in Eq. G2. The zero energy states in the remaining panels are highly degenerate; their counting matches with that of the corresponding $(N, 2Q^*)$ system of non-interacting fermions with the lowest two LLs taken as degenerate.

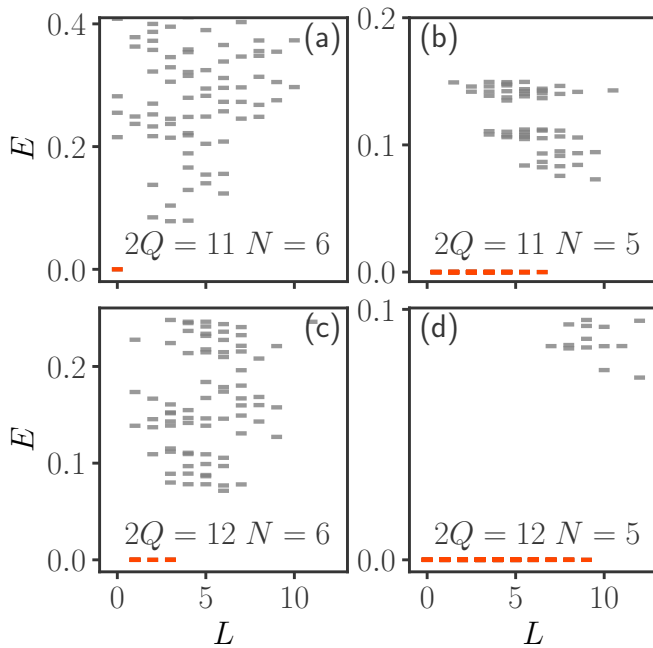


FIG. 6. Spectra for the Trugman-Kivelson interaction for several $(N, 2Q)$ systems (same as in Fig. 3) obtained by exact diagonalization. Only two lowest Landau levels are included, which are assumed to be degenerate. Zero energy states are shown in orange. The energy is quoted in arbitrary units (set by the KT interaction), but all four plots are in the same units.

-
- ¹ R. Wooten and J. Macek, in *APS March Meeting Abstracts* (2015), vol. 2015 of *APS Meeting Abstracts*, p. D5.003.
- ² T. T. Wu and C. N. Yang, *Physical Review D* **16**, 1018 (1977).
- ³ T. T. Wu and C. N. Yang, *Nucl. Phys. B* **107**, 365 (1976).
- ⁴ DLMF, *NIST Digital Library of Mathematical Functions*, <http://dlmf.nist.gov/>, Release 1.0.26 of 2020-03-15, f. W. J. Olver, A. B. Olde Daalhuis, D. W. Lozier, B. I. Schneider, R. F. Boisvert, C. W. Clark, B. R. Miller, B. V. Saunders, H. S. Cohl, and M. A. McClain, eds., URL <http://dlmf.nist.gov/>.
- ⁵ G. W. Stewart, *SIAM Journal on Matrix Analysis and Ap-*

- plications* **23**, 601 (2002).
- ⁶ J. K. Jain, *Composite fermions* (Cambridge University Press, 2007).
- ⁷ S. A. Trugman and S. Kivelson, *Phys. Rev. B* **31**, 5280 (1985), URL <https://link.aps.org/doi/10.1103/PhysRevB.31.5280>.
- ⁸ J. K. Jain, *Phys. Rev. B* **41**, 7653 (1990).
- ⁹ E. H. Rezayi and A. H. MacDonald, *Phys. Rev. B* **44**, 8395 (1991), URL <http://link.aps.org/doi/10.1103/PhysRevB.44.8395>.